



**Fermilab-Conf-08-146-APC May 2008**

**RADIATION SHIELDING FOR THE MAIN INJECTOR COLLIMATION SYSTEM\*\*†**

**Igor Rakhno**

Fermilab, P.O. Box 500, Batavia, IL 60510, USA

**Abstract**

The results of Monte Carlo radiation shielding studies performed with the MARS15 code for the Main Injector collimation system at Fermilab are presented and discussed. MAD-to-MARS Beam Line Builder is used to generate realistic extended curvilinear geometry models.

---

\*Work supported by Fermi Research Alliance, LLC under contract No. DE-AC02-07CH11359 with the U.S. Department of Energy.

†Work presented at the 9<sup>th</sup> Workshop on Shielding Aspects of Accelerators, Targets and Irradiation Facilities (SATIF-9), April 21-23, 2008, Oak-Ridge, Tennessee, USA.

## Introduction

A Proton Plan was developed recently at Fermilab for the benefit of the existing neutrino programs as well as to increase anti-proton production for Tevatron programs [1]. As a part of the plan, the intensity of proton beams in the Main Injector (MI) should be increased by means of slip-stacking injection. In order to localize beam loss associated with the injection, a collimation system was designed [2] that satisfies all the radiation and engineering constraints. The system itself comprises a primary collimator and four secondary ones to which various masks are added. It is calculated that beam loss at the slip-stacking injection is equal to 5% of total intensity which is  $5.5 \times 10^{13}$  protons per pulse. As far as pulse separation is 2.2 seconds, one has  $1.25 \times 10^{12}$  protons interacting per second with the primary collimator. In the paper the geometry model of the corresponding MI region and beam loss model are described. The model of the 200-m region was built by means of the MAD-MARS Beam Line Builder (MMLB) [3] using results of previous collimation studies. The results of radiation shielding calculations performed with the MARS15 code [4] are presented.

## Geometry Model of the Region

Fragments of the geometry model developed for the MI collimation region are shown in Figures 1-3. The model extends from Q230 quadrupole up to Q310, *i.e.* for about 200 meters, and includes all essential elements with detailed description of geometry and materials [5]. The MI tunnel with concrete walls is surrounded by gravel, while there is clay under the floor. Detailed two-dimensional distributions of magnetic field in the dipoles and quadrupoles were calculated with the OPERA-2D code [6].

Each of the secondary collimators (see Figure 2) has a steel core covered with marble layers to shield residual activity [7]. Only surfaces that are easy to reach are covered with marble: front, rear,

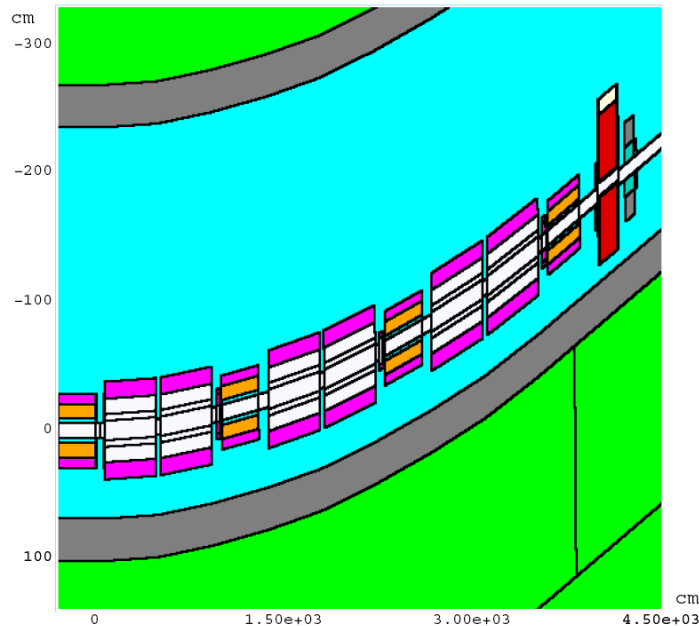


Figure 1. Fragment of the model from Q230 quadrupole up to the first secondary collimator S1.

left side, and left top. For each of the secondary collimators, the jaws were aligned precisely according to the results of the collimation studies [2, 7]. In addition, each of the collimators but S4 has two masks: a polyethylene mask upstream and steel/concrete mask downstream. The last collimator, S4, needs only the mask downstream. The masks are used to absorb radiation scattered in backward and forward direction and, therefore, provide extra protection.

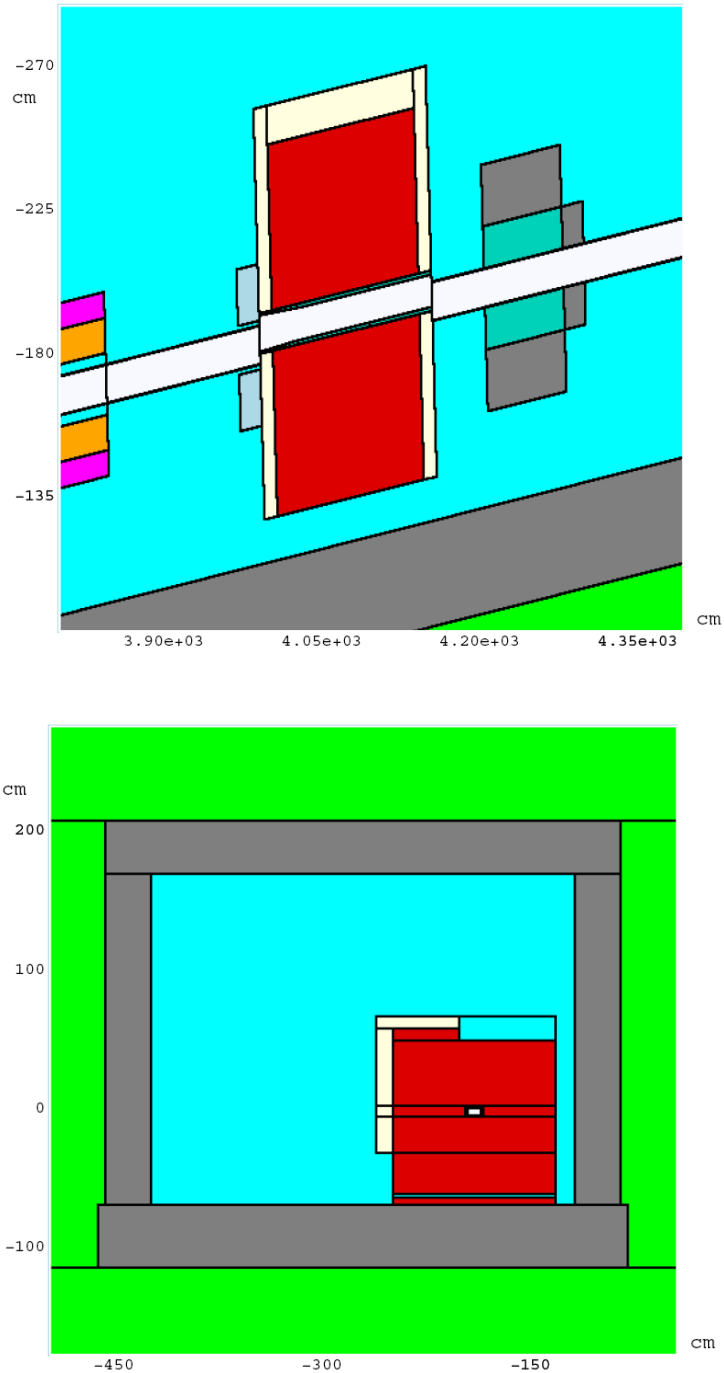


Figure 2. Geometry model of the first secondary collimator S1: plan view with upstream and downstream masks (top) and cross section (bottom).

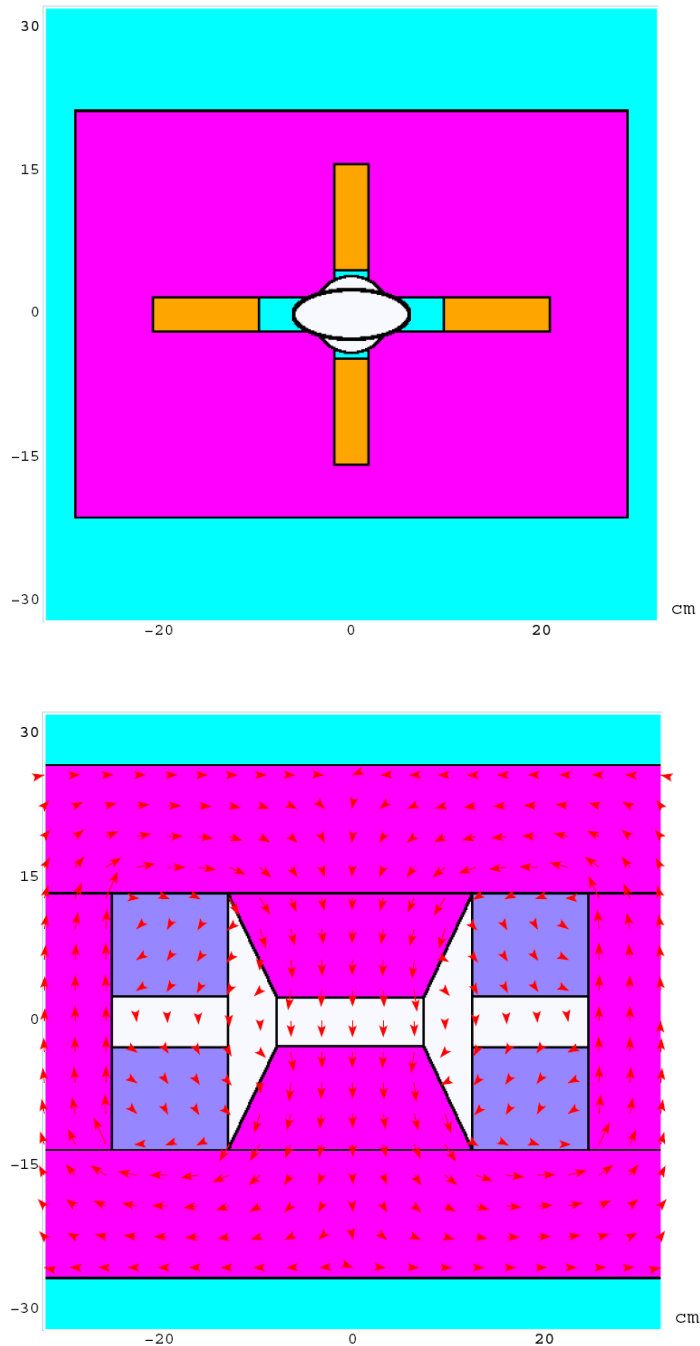


Figure 3. Cross section of the model of a quadrupole (top) and bending dipole (bottom). Magnetic field is shown with arrows only for the dipole.

An electron cooling system is installed in the region from Q305 up to Q307. In order to protect the sensitive equipment against scattered radiation, a concrete wall (100 cm in length, 136 cm in width, and 152 cm in height) is required upstream of Q305.

All quadrupoles in the region have the same design, so that the same geometry model is used (see Figure 3). Only lengths and magnetic fields can differ. The same statements apply to bending dipoles in the region. There are several horizontal and vertical trim dipoles in the beam line. It is assumed that,

during the slip-stacking injection, magnetic field in most trim dipoles is equal to zero [2]. Therefore, in the model the trim dipoles, each 30.5 cm in length, serve only for the purpose of absorption of scattered radiation.

In addition, the beam line includes also four horizontal trim dipoles with non-zero magnetic field upstream of the following quadrupoles: Q302, Q304, Q306, and Q308. However, the beam line is built by means of the MMBLB with the magnetic field in these trim dipoles turned off. For subsequent calculations of the beam loss and radiation transport in the region, the magnetic field is turned on.

### Model of Beam Loss on the Collimators

The two-stage collimation system designed for the slip-stacking injection in MI [2] comprises a single-jaw horizontal primary collimator (tungsten bar 0.25 mm in thickness placed downstream of Q230) and four secondary collimators S1 thru S4 with 5.08 cm X 10.16 cm rectangular stainless steel apertures (Figures 1 and 2). A detailed description of alignment of the collimators is given in [2]. As far as the beam loss is very sensitive to alignment of the collimators and other beam line elements, one uses the spatial beam loss distribution on the secondary collimators calculated with the STRUCT code [2] as a source for subsequent Monte Carlo modeling of radiation transport with the MARS code. The calculated data on integral beam loss on the secondary collimators is given in Table 1. It should be noted that, according to the STRUCT results, 99.7% of total beam loss occurs inside the collimation region and 87.3% out of the 99.7% occurs on the four secondary collimators while the remaining 12.4% is lost on the beam pipe and other elements. In order to perform conservative calculations, one assumes that 100% of the beam loss occurs on the four secondary collimators.

Table 1. Breakdown of the calculated integral beam loss on the secondary collimators. Here 100% corresponds to  $1.25 \times 10^{12}$  protons interacting with the primary collimator per second.

Collimator	Beam loss (%)
S1	28
S2	40
S3	10
S4	22
Total	100

### Results of Calculations

#### *Surface water activation*

Activation of water with radionuclides is strictly limited by environmental protection regulations. In the calculations of surface water activation one follows the procedure developed at Fermilab and referred to as *Fermilab Concentration Model* (see [8-9] and references therein). The procedure consists in determining the average star density over a so-called 99%-volume of soil surrounding the tunnel. The volume should be big enough in order to satisfy the following condition: the calculated star density on external boundary of the volume should be at the level of 1% when compared to the calculated maximum star density on internal boundary, *i.e.* tunnel-soil interface. Either maximum star density at the tunnel-soil interface,  $S_{max}$ , or star density averaged over such a 99%-volume,  $\langle S \rangle$ , can be used with the *Concentration Model*. Numerous studies showed that the following simple relation

holds:  $\langle S \rangle = S_{\max}/50$ , where the factor of 50 was confirmed in various independent calculations ( $S_{\max}$  and  $\langle S \rangle$  were calculated independently in this study).

The calculated distributions of star density around the region are shown in Figure 4. The model of beam loss described in the previous section eventually gives rise to the star density distribution from S1 up to Q310. In order to calculate the distribution upstream of the latter region, *i.e.* from Q230 up to Q301, one needs to consider primary collimator as the initial source of beam loss. A separate calculation was performed with such a source for the region from Q230 up to Q301. The highest calculated star densities are observed around the secondary collimators S1, S2, and S4. The distribution around the hottest spot–collimator S2–is also shown in Figure 4. The calculated average star densities are given in Table 2. There are underdrains all along the MI tunnel and suitably placed sump pumps and generation of radionuclides in surface water is of primary concern. Taking into account a realistic operational schedule and operational efficiency, annual amount of protons is expected to be  $3.7 \times 10^{20}$  [10]. In such a case after a year of operation the *Concentration Model* gives rise to the following activation around the hottest spot (secondary collimator S2): surface water - 32% of total limit; ground water (aquifer) - much less than 1% of total limit.

Table 2. The calculated star densities  $\langle S \rangle$  ( $\text{cm}^{-3}\text{s}^{-1}$ ) averaged over corresponding 99%-volumes around the secondary collimators S1, S2, and S4.

$\langle S1 \rangle$	330
$\langle S2 \rangle$	460
$\langle S4 \rangle$	280

### ***Dose load to magnet coils***

Lifetime of a magnet depends to a great extent on the dose accumulated in its coils. The most vulnerable material in the coils is epoxy which can stand absorbed dose up to 4 MGy [11]. The highest dose–up to 1 MGy per year–is observed in coils of the Q301 quadrupole which is upstream of the secondary collimator S1. For the magnet this means the lifetime of about four years. For all the other dipoles, trim dipoles, and quadrupoles the absorbed dose in the hottest spot varies from 0.1 up to 0.5 MGy/yr which means the lifetime of about 8 years and more.

Two marble masks, each 10 cm in thickness, are placed on downstream face of the quadrupole Q230 and upstream face of the dipole IDC011. The masks protect coils against radiation scattered on the primary collimator and backscattered from the dipole IDC011 as well as enable us to reduce residual activation of the magnets.

In Figure 5 one can see the extended tail in forward direction due to scattering on the secondary collimators as well as significant backscattered component. In order to reduce the radiation scattered in forward direction (mostly low-energy neutrons), masks consisting of a steel core surrounded with concrete (total thickness of 75 cm) are placed downstream of the secondary collimators (Figure 2). As to the absorbed dose, such a steel and concrete mask provides an extra absorption factor of about four. In response to these calculations (but not included in this report) an additional mask was placed downstream of S1, S2 and S4 but just upstream of the next machine element (H302, K304, V309) as described in Ref. [12]. Intensity of the backscattered radiation from the collimators can be reduced by means of the polyethylene masks 18 cm in thickness placed upstream of the collimators. The polyethylene masks provide an extra absorption factor of about three.

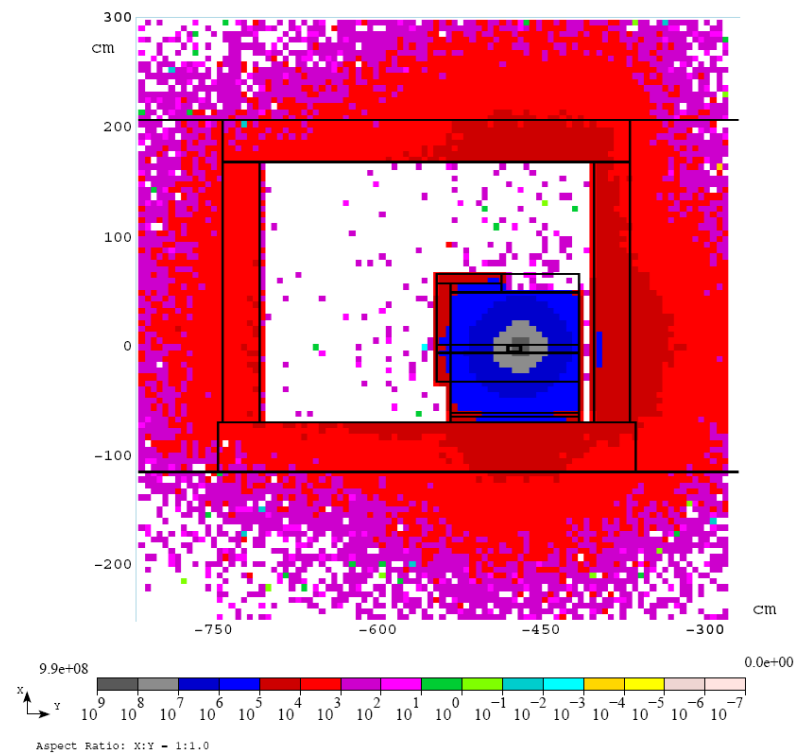
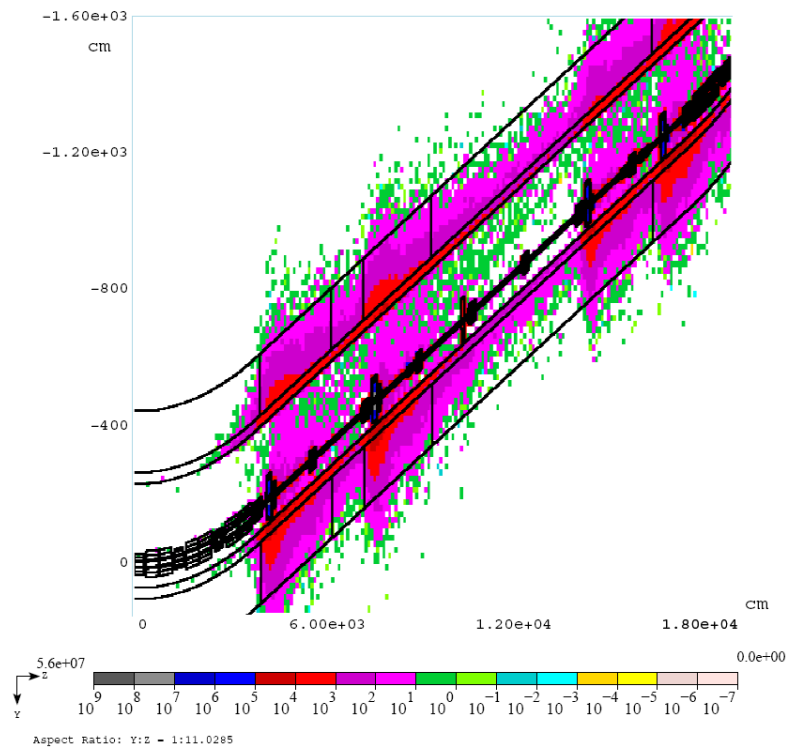


Figure 4. Calculated distributions of star density ( $\text{cm}^{-3} \text{s}^{-1}$ ) from S1 up to Q310 (plan view, top) and around S2 (cross section, bottom).

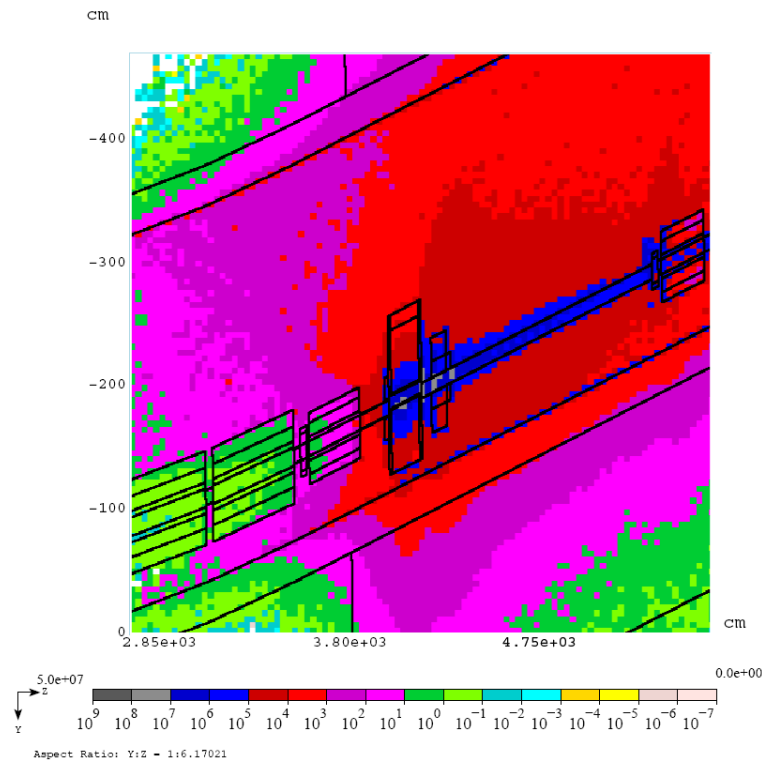


Figure 5. Calculated distribution (plan view) of absorbed dose (Gy/yr) around the first secondary collimator S1.

### *Distribution of residual activity*

Restrictions on residual activation of beam line components and tunnel are derived mostly from practical considerations. When planning on various maintenance and hands-on procedures, usually after a 30-day irradiation and 1-day cooling the residual dose is not to exceed 100 mrem/hr at a distance of 30 cm from the surface [11]. The calculated distributions of residual dose around the secondary collimator S2 corresponding to the required irradiation and cooling time are shown in Figure 6. There are several small—with linear dimension of about 10 cm—hot spots around Q232, V301, Q301, and Q302. The spots reveal residual dose above 1 rem/hr and the highest dose is observed around the beam pipe. Provided the distance between the magnets in the region from Q230 up to Q301 is small, the issue of high residual activity can be resolved by means of a local shielding such as bags with poly-beads, sand *etc.*

About 70% of the total beam loss in the collimation region occurs on the first two secondary collimators, S1 and S2. As a consequence, the hottest spots are observed inside the collimators (see Figure 6). In order to reduce the contact residual dose on the surface of the collimators down to an acceptable level, the bodies of all the secondary collimators—front, rear, and part of side surface—are covered with marble layers 10 cm in thickness (Figures 1 and 2). The advantage of using marble is in its extremely low residual activation while providing significant absorption of MeV gammas generated in the steel core [7]. One can see from Figure 6 that the hottest spots around S2 are the following: (i) 70 mrem/hr on the wall at the beam line elevation ( $X=0$ ); (ii) 110 mrem/hr atop the S2 itself.

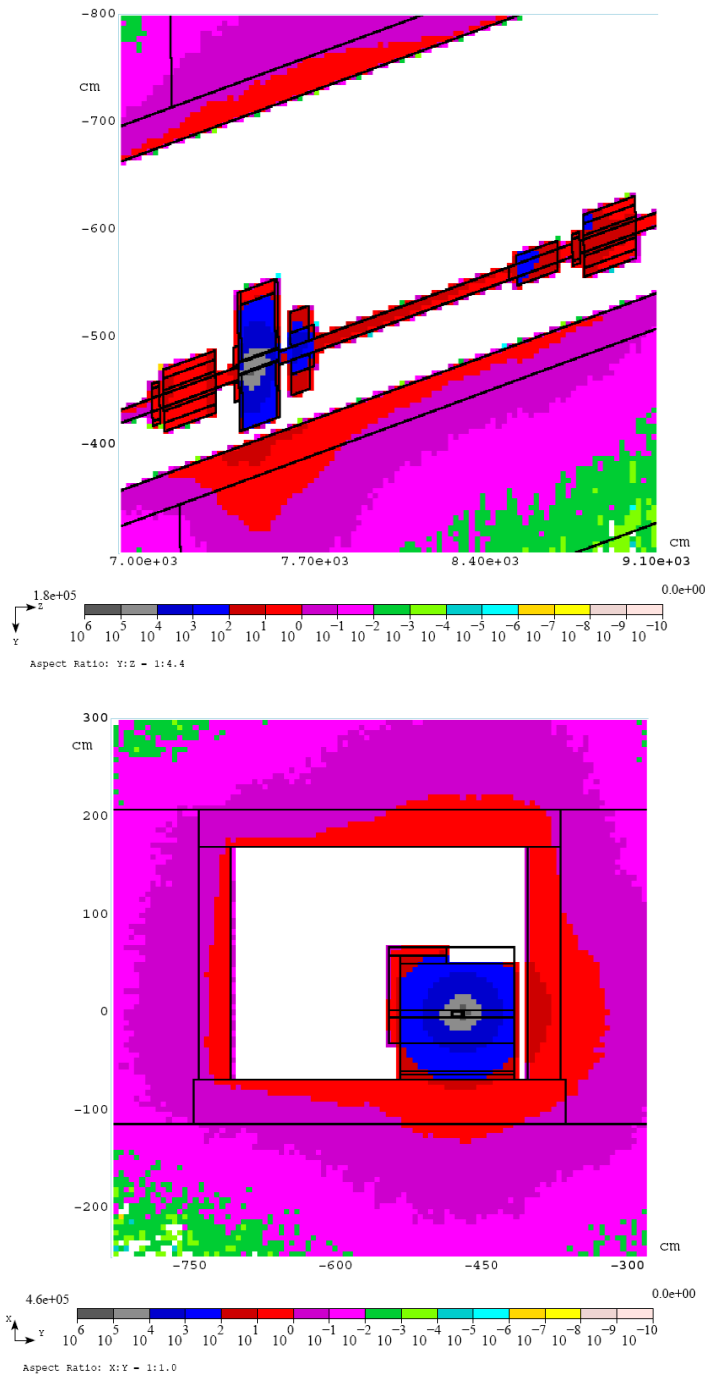


Figure 6. Calculated distributions of contact residual dose (mrem/hr) around the secondary collimator S2: plan view (top) and cross section (bottom).

## Conclusions

The radiation shielding studies were performed for the MI collimation system that comprises a primary horizontal collimator and four secondary ones. The following problems were addressed: (i) surface water activation; (ii) dose load to magnet coils; (iii) distribution of residual activity around the

region. It was shown that after a year of operation the activation of surface water around the hottest spot—secondary collimator S2—is about 32% of total limit. Activation of groundwater (aquifer) is negligible—much less than 1% of total limit. The highest dose—up to 1 MGy per year—is observed in coils of the Q301 quadrupole which is upstream of the secondary collimator S1. For the magnet this means the lifetime of about four years. For all the other bending dipoles, trim dipoles, and quadrupoles the absorbed dose in the hottest spot varies from 0.1 up to 0.5 MGy/yr which means the lifetime of about eight years and more. The predicted residual activity around the region reveals several small hot spots between Q230 and Q302. The issue can be resolved by means of a local shielding. Marble layers are used to cover the external surface of the secondary collimators and reduce the residual dose down to an acceptable level. More details can be found in Ref. [13].

## References

- [1] “The Proton Plan,” Beams-doc-1441-v1 (2004).
- [2] A.I. Drozhdin, B.C. Brown, D.E. Johnson, K. Koba, I. Kourbanis, N.V. Mokhov, I.L. Rakhno, V.I. Sidorov, “Collimation System Design for Beam Loss Localization with Slipstacking Injection in the Fermilab Main Injector,” Fermilab-Conf-07-249-AD (2007).
- [3] M.A. Kostin, O.E. Krivosheev, N.V. Mokhov, I.S. Tropin, “An Improved MAD-MARS Beam Line Builder: User's Guide,” Fermilab-FN-0738-rev (2004).
- [4] N.V. Mokhov, Fermilab-FN-628 (1995); N.V. Mokhov *et al.*, *Rad. Prot. Dosimetry*, **116** (2005) 99; N.V. Mokhov *et al.*, *Int. Conf. on Nucl. Data Sci. Technology*, AIP Conf. Proc., **769** (2005) 1618; N.V. Mokhov, S.I. Striganov, “MARS15 Overview,” *Hadronic Shower Simulation Workshop*, AIP Conf. Proc., **896** (2006) 50; <http://www-ap.fnal.gov/MARS/>.
- [5] B.C. Brown, N.V. Mokhov, Private communication, Fermilab (2007).
- [6] J.-F. Ostiguy, Private communication, Fermilab (2007).
- [7] N.V. Mokhov and B.C. Brown, “MARS15 Calculations for MI8 Collimator Design,” Fermilab-TM-2359-AD (2006).
- [8] “Fermilab Radiological Control Manual,” <http://www-esh.fnal.gov/FRCM/>.
- [9] J.D. Cossairt, “Use of a concentration-based model for calculating the radioactivation of soil and groundwater at Fermilab,” Fermilab Note EP-8; J.D. Cossairt, A.J. Elwyn, P. Kesich, A. Malensek, N. Mokhov, and A. Wehmann, “The concentration model revisited,” Fermilab Note EP-17; [http://www-esh.fnal.gov/pls/default/esh\\\_home\\\_page.page?this\\\_page=11013/](http://www-esh.fnal.gov/pls/default/esh\_home\_page.page?this\_page=11013/).
- [10] I. Kourbanis, Private communication, Fermilab (2007).
- [11] O.E. Krivosheev, N.V. Mokhov, “The Proton Driver Design Study,” Chapter 10, Fermilab, TM-2136 (2000).
- [12] B.C. Brown, “Main Injector Collimation System Hardware,” Beams-doc-2881 (2007).
- [13] I. Rakhno, “Radiation shielding for the Main Injector collimation system,” Fermilab-TM-2391 (2007).